DARTS-well

An Open-Source Coupled Wellbore-Reservoir Numerical Model for Subsurface CO_2 Sequestration

Moslehi, S.; Voskov, D.

DOI
10.2118/223892-MS

Publication date
2025

Document Version
Final published version

Published in
Society of Petroleum Engineers - SPE Reservoir Simulation Conference, RSC 2025

SPE-223892-MS

DARTS-well: An Open-Source Coupled Wellbore-Reservoir Numerical Model for Subsurface CO_2 Sequestration

S. Moslehi, TU Delft; D. Voskov, TU Delft, Stanford University

This paper was prepared for presentation at the SPE Reservoir Simulation Conference held in Galveston, Texas, USA, 25–27 March 2025.

Abstract

Subsurface CO_2 sequestration is a promising method to advance carbon neutrality and support the shift toward sustainable energy. However, the unique behavior of CO_2 in these operations, particularly for cold CO_2 injection in depleted hydrocarbon reservoirs, poses challenges to wellbore injectivity, reservoir containment, and reservoir capacity. These challenges necessitate the development of a numerical model to better understand and optimize the interplay between wellbore dynamics and reservoir processes. In this work, we present the development of an open-source coupled wellbore-reservoir numerical model, named DARTS-well, which is tailored to CO_2 disposal in subsurface reservoirs. To this end, a multi-segment, multi-phase, non-isothermal wellbore model is first developed using the Drift-Flux Model (DFM), and its results for selected CO2 injection scenarios are validated against the commercial transient wellbore simulator OLGA. The multi-segment wellbore model is then coupled with the Delft Advanced Research Terra Simulator (DARTS) which is used in this study as the reservoir simulator. DARTS is widely used and validated for energy transition applications. The coupled model utilizes the Operator-Based Linearization (OBL) technique, employing state-dependent operators for thermodynamic properties interpolated from predefined tables or generated on the fly. This OBL parametrization approach addresses challenges associated with complex physics and reduces computational time, making it well-suited for modeling subsurface CO_2 sequestration.

Introduction

Carbon dioxide (CO_2) capture from surface sources and its sequestration in subsurface reservoirs, also known as Carbon Capture and Sequestration (CCS), is a promising approach to advance carbon neutrality and support the shift toward sustainable energy. However, the unique behavior of CO_2 in these operations, particularly for cold CO_2 injection in depleted hydrocarbon reservoirs, poses challenges to wellbore injectivity, reservoir containment, and reservoir capacity. These challenges necessitate the development of a numerical model to better understand and optimize the interplay between wellbore dynamics and reservoir processes. Ignoring these wellbore processes in CCS operations can result in inaccurate predictions of bottom-hole pressure and temperature, and an oversimplified representation of the wellbore-reservoir interactions, undermining the reliability of numerical reservoir simulators.

The standard well model is the most commonly used approach for modeling wells in reservoir simulations. It treats the well as an internal boundary condition or a source/sink term within the perforated reservoir blocks (Ertekin et al., 2001). While providing computational efficiency, this model has significant limitations. It overlooks the physics within the wellbore, including multi-phase flow, thermal effects, and changes in CO_2 properties under varying thermodynamic conditions. Van Nimwegen et al. (2023) expresses the need for coupled wellborereservoir modeling for CO_2 operations from two perspectives. From a flow assurance perspective, traditional reservoir models often approximate the reservoir's behavior using a constant Productivity Index (PI), neglecting dynamic thermal and hydraulic interactions of the surrounding formation with the wellbore. From the reservoir modeling perspective, inflow is typically modeled with fixed temperature or enthalpy, or using lift tables, which fail to account for significant thermal and hydraulic changes within the wellbore (Livescu et al., 2010). For instance, for injection of cold CO_2 into depleted hydrocarbon reservoirs, using the tubing head temperature as the bottom-hole temperature for reservoir simulators can be misleading, as CO_2 undergoes temperature changes along the wellbore, resulting from heating due to the geothermal gradient and some cooling caused by CO_2 expansion (Joule-Thomson effect). Such variations directly affect the temperature of CO_2 injected into the formation at the sandface, thereby influencing near-wellbore and reservoir conditions (Zamani et al., 2024; Indina et al., 2024; Castaneda et al., 2025). By integrating the wellbore with the reservoir model, we can capture these effects more accurately, improving the simulation's reliability. This coupled modeling approach enables detailed investigations of CO_2 injection scenarios involving transient periods such as well start-up, well shut-in, and intermittent CO_2 injection due to variable supply or ship-transport systems. Furthermore, it facilitates the study of operational challenges, including leaky legacy wells (Pan et al., 2011a; Pan and Oldenburg, 2020; Hu et al., 2012), CO_2 well blowouts (Oldenburg and Pan, 2020), and injection into layered reservoirs (Rasmusson et al., 2015; Abdelaal and Zeidouni, 2023), providing insights for CO_2 sequestration operations.

To model multi-phase fluid flow in pipes (e.g., wells), various approaches are used in the literature. Equivalent Porous Medium (EPM) model or Equivalent Permeability Model (EPM) is the simplest approach for modeling fluid flow in pipes which considers the pipe as a porous medium (Moridis et al., 2022; Pour et al., 2023). It uses Darcy's law as the momentum equation to calculate fluid velocity in the pipe considering a porosity value equal to 1, a very high permeability, and no capillary pressure for multi-phase fluid flow. This model has shown deviations when used to describe CO_2 leakage flow in the wellbore due to not including inertial forces (Feng et al., 2017; Hu et al., 2012; Cai et al., 2024). Unlike EPM, the Multi-Fluid Model (MFM) considers the pipe as an actual void space and so uses the Navier-Stokes equation as the momentum equation to calculate phase velocities. In this model, a momentum equation is written for each phase present in the pipe.

Similar to MFM, the Drift-Flux model (DFM) model also considers the pipe as an actual void space, but instead of having multiple momentum equations, a single momentum equation is written for the mixture as a whole, and a slip relation is used to account for the relative motion of liquid and gaseous phases. Therefore, DFM is an approximate formulation compared to the more rigorous multi-fluid model. However, it is of considerable importance because of its simplicity and easy applicability to a wide range of multi-phase flow problems of practical interest (Goda et al., 2003). The homogeneous model is a simplified form of the DFM model considering no slip between the phases in the pipe. Therefore, it is suitable for the cases where the phases have similar density values (near the critical point) (Hammer et al., 2021).

Comparison of the MFM and DFM models highlights several advantages of the latter (Spesivtsev et al., 2013). First, the DFM model employs a single momentum equation, reducing computational requirements compared to the MFM model. Second, the DFM model features smooth and differentiable closure relations, which enhance numerical stability and robustness. These relations are calibrated using laboratory data for vertical and inclined flows and remain free from singularities at low-volume fractions. In contrast, the MFM model may encounter numerical instabilities, such as the unrealistic growth of velocity when a phase disappears. Furthermore, the MFM model introduces mathematical complexities and uncertainties in defining interfacial interaction terms between phases. While the DFM model also relies on empirical correlations for parameters such as drift velocity and profile parameter, this disadvantage is less pronounced than the MFM model.

Because of the discussed inherent difficulties in modeling multi-phase flow with MFM and limitations in the accuracy of the EPM model, the two-phase DFM model presented by Pan et al. (2011b), which is the modified version of the two-phase DFM model originally presented by Shi et al. (2005), is used in this study. The developed multi-segment wellbore model is then coupled with the Delft Advanced Research Terra Simulator (DARTS), a widely used and validated reservoir simulator for subsurface energy transition applications (Wang et al., 2020; Wapperom et al., 2024; Ahusborde et al., 2024).

Methodology

In this section, we first describe how the multi-segment wellbore model is developed, and at the end, we will deal with the coupling of the wellbore model with the open-DARTS reservoir model.

Wellbore model: Introduction to the two-phase drift-flux model

The drift-flux model for two-phase flow describes the slip between gas and liquid as a combination of two mechanisms. One mechanism results from the non-uniform profiles of velocity and phase distribution over the pipe cross section. The other mechanism results from the tendency of gas to rise vertically through the liquid due to buoyancy. Shi et al. (2005) presented a formulation that combines the two mechanisms, and it relates the gas velocity to the mixture velocity using two empirical parameters: profile parameter (or distribution parameter or coefficient) and the gas drift velocity. The overall approach of the two-phase drift-flux model involves three key steps. First, the mixture velocity at cell interfaces is obtained by solving the momentum equation of fluid mixture at each interface. Second, the profile parameter and drift velocity are calculated using empirical relationships. Finally, the gas velocity and liquid velocity are determined primarily as functions of the mixture velocity, the profile parameter, and the drift velocity. The phase velocities are then used in the advective flux term of the mass and energy conservation equations. Further description and derivation of the drift-flux model is given in detail by Shi et al. (2005) and Pan and Oldenburg (2014). In this work, the gas velocity (υ_g) and liquid velocity are calculated using the following relationships

$$\upsilon_g = C_0 \frac{\rho_m}{\rho_m^*} \upsilon_m + \frac{\rho_l}{\rho_m^*} \upsilon_d, \tag{1}$$

$$\upsilon_l = \frac{(1 - s_g C_0)\rho_m}{(1 - s_g)\rho_m^*} \upsilon_m - \frac{s_g \rho_g}{(1 - s_g)\rho_m^*} \upsilon_d, \tag{2}$$

where C_0 is the profile parameter, ρ_m and $\rho^*{}_m$ are the average density and the profile-adjusted average density, υ_m is the mixture velocity, ρ_l is liquid density, υ_d is the drift velocity, and s_g is gas saturation. The evaluations of these parameters are provided by Pan (2011) and are not repeated here for brevity.

Wellbore model: Implementation of the mathematical formulation

The mass- and energy-conservation equations are discretized in space using the finite-volume scheme and in time using using a backward, first-order, Euler scheme. The scalar variables such as pressure, overall mole fractions, and temperature are evaluated at segments centroids, while velocities are computed at segments interfaces.

The discretization of the momentum equation is implemented semi-implicitly, similar to T2Well (Pan and Oldenburg, 2014). The discretized momentum equation at the interface 23 between two neighboring wellbore segments 2 and 3 in Figure 1 can be written as

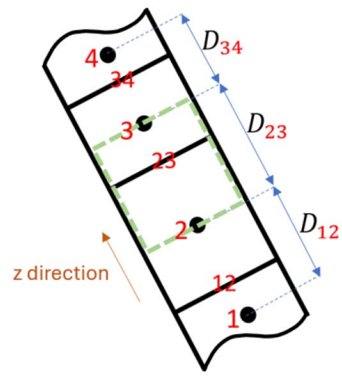

Figure 1—Indexing of control volumes and their interfaces for a wellbore.

$$\frac{(\rho_m \upsilon_m - \rho_m^n \upsilon_m^n)_{23}}{\Delta t} + \frac{\delta_3^n - \delta_2^n}{A_{23}(z_3 - z_2)} = -\left(\frac{\Gamma f^n \rho_m \upsilon_m |\upsilon_m^n|}{2A}\right)_{23} - \frac{p_3 - p_2}{z_3 - z_2} - (\rho_m)_{23} g\cos(\theta_{23}), \tag{3}$$

where δ_2 and δ_3 are the momentum term at the 2nd and 3rd segments, which is defined as the weighted-average of that at all neighboring interfaces. For example, δ_2 is

$$\delta_2 = \frac{(A_{12}\delta_{12})/D_{12} + (A_{23}\delta_{23})/D_{23}}{A_{12}/D_{12} + A_{23}/D_{23}}, \tag{4}$$

where δ_{12} and δ_{23} are momentum terms at interfaces 12 and 23.

Finally, from Equation 3, the product of mixture density and velocity at interface 23 at the current time step is calculated as

$$(\rho_m v_m)_{23} = -\frac{w}{z_3 - z_2}(p_3 - p_2) - wg\cos(\theta_{23})(\rho_m)_{23} - w\left(\frac{\delta_3^n - \delta_2^n}{A_{23}(z_3 - z_2)} - \frac{(\rho_m^n v_m^n)_{23}}{\Delta t}\right), \tag{5}$$

where

$$w = \frac{1}{1/\Delta t + (\Gamma f^n |\upsilon_m^n|)_{23}/(2A_{23})}. \tag{6}$$

The phase velocities at interface 23 at the current time step, $(\upsilon_g^{n+1})_{23}$ and $(\upsilon_l^{n+1})_{23}$, are then calculated using the following equations with both the drift velocity and the profile parameter evaluated at the previous time level:

$$(\upsilon_g)_{23} = \left(\frac{C_0^n}{\rho_m^*}(\rho_m \upsilon_m) + \frac{\rho_l}{\rho_m^*}\upsilon_d^n\right)_{23}, \tag{7}$$

$$(\upsilon_l)_{23} = \left(\frac{1 - C_0^n s_g}{(1 - s_g)\rho_m^{*n+1}}(\rho_m \upsilon_m) - \frac{s_g \rho_g}{(1 - s_g)\rho_m^*}\upsilon_d^n\right)_{23}. \tag{8}$$

The discretized mass conservation equation of the c^{th} component for segment 3 is given below (the velocities at both interfaces of segment 3 are needed to calculate mass advection rate into or out of the control surface).

$$V_3\left[\left(\sum_{j=1}^{np} s_j\rho_j x_{cj}\right)-\left(\sum_{j=1}^{np} s_j\rho_j x_{cj}\right)^n\right]_3+\Delta t\sum_{l=23,34}\left(\sum_{j=1}^{np}\upsilon_j^l A^l s_j^{l,\,\mathrm{up}}\,\rho_j^{l,\,\mathrm{up}}\,x_{cj}^{l,\,\mathrm{up}}\right)+\Delta t q_{c,3}=0,\qquad c=1,\ \ldots,\ n_c. \tag{9}$$

Knowing that $U_j = h_j - p/\rho_j$, the discretized energy conservation equation for segment 3 is given below.

$$\begin{aligned} &V_3\left[\left(\sum_{j=1}^{np} s_j\rho_j\left(h_j+\frac{\left(\upsilon_j^2\right)^n}{2}+gz\cos(\theta)\right)-p\right)-\left(\sum_{j=1}^{np}\left(s_j\rho_j\right)^n\left(\left(h_j\right)^n+\frac{\left(\upsilon_j^2\right)^n}{2}+gz\cos(\theta)\right)-p^n\right)\right]_3 \\ &+\Delta t\sum_{l=23,34}\left[\sum_{j=1}^{np}A^l s_j^{l,\,\mathrm{up}}\,\rho_j^{l,\,\mathrm{up}}\left(\upsilon_j^l h_j^{l,\,\mathrm{up}}+\left(\upsilon_j^l\right)^n\left(\frac{\left(\left(\upsilon_j^l\right)^2\right)^n}{2}\right)^{up}+\left(\upsilon_j^l\right)^n\left(gz^l\cos(\theta^l)\right)^{up}\right)\right]+\Delta t q_{\mathrm{heat},3}=0. \end{aligned} \tag{10}$$

Besides the explicit spatial acceleration terms used in solving the momentum equation, T2Well also considers all the velocities used in calculation of kinetic and potential energy in the energy conservation equation explicitly to avoid unnecessarily slow convergence. In the flux term, in addition to the phase saturation, phase density, and phase enthalpy, phase specific kinetic energy and potential energy (the amount of which is independent of the phase type) should be upwinded to increase the numerical stability (Tonkin et al., 2023).

Coupled wellbore-reservoir model: Implementation of the mathematical formulation

In this study, Delft Advanced Research Terra Simulator (DARTS) is used as the reservoir simulator and as the platform to solve the system of wellbore governing equations for the coupled model. DARTS is a robust and computationally-efficient simulator which can be used to model various energy transition problems. In the framework of DARTS, the evaluation of the residuals and construction of the Jacobian matrix are done using the operator-based linearization (OBL) approach (Voskov, 2017). In this approach, appropriate state-dependent properties are grouped together as state-dependent operators, and these operators are interpolated from predefined tables (static parametrization) or generated on the fly during the simulation (adaptive parametrization). The OBL approach also provides an opportunity to control the non-linearity in physics by changing the resolution of parameter space, increasing performance, flexibility, and robustness of simulation (Khait and Voskov, 2017).

To include and solve the wellbore governing equations in open-DARTS, we first write the discretized mass conservation equation (Equation 9) in the operator general form as follows

$$V_i\,\phi_{0i}\left[\alpha_c(\omega)-\alpha_c\left(\omega^n\right)\right]_i+\Delta t\sum_{l\in L(i)}\sum_{j=1}^{np} q_j\beta_{cj}\left(\omega^{l,up}\right)+\Delta t q_{c,i}=0,\qquad c=1,\ \ldots,\ n_c, \tag{11}$$

where ω and ω^n represent the primary variables at the current and previous time steps, respectively. Here we defined the state-dependent operators α and β as

$$\alpha_c(\omega)=\sum_{j=1}^{np} s_j\rho_j x_{cj},\qquad \beta_{cj}(\omega)=\rho_j x_{cj},\qquad c=1,\ \ldots,\ n_c,\qquad j=1,\ \ldots,\ n_p. \tag{12}$$

Besides, we need to introduce phase volumetric rate qj which will be defined for the reservoir as

$$q_j=\Gamma^l\lambda_j(\omega)\Delta\psi_j^l,\qquad \lambda_j(\omega)=\frac{k_{rj}}{\mu_j},\qquad j=1,\ \ldots,\ n_p, \tag{13}$$

where Γ^l is the geometric part of transmissibility for interface l, λ_j is the phase mobility, k_{rj} and μ_j are phase relative permeability and viscosity, respectively, and $\Delta\psi_j^l$ is the phase pressure potential based on Darcy's law. For wellbore, the phase volumetric rate is calculated based on gas and liquid velocities from the DFM model in Equations 7 and 8, respectively.

Equation 11 is a generic equation for both reservoir and wellbore with only the difference in q_j term. Depending on the connection type, phase volumetric rates from the DFM model are used for wellbore segment connections, Darcy's law is applied for reservoir cell connections, and a modified form of Darcy's law using the Peaceman model is employed for connections between reservoir cells and wellbore segments. Notably, when solving the equation for a wellbore segment, the porosity in the accumulation term is equal to 1. The discretized energy conservation equation (Equation 10) has not yet been implemented in the coupled wellbore-reservoir model,and is still ongoing work.

Validation of the wellbore model

This section presents several examples of the developed stand-alone wellbore model and validation of them against the commercial wellbore simulator OLGA.

Non-isothermal single-phase (gas) single-component (CO_2) fluid flow in a vertical wellbore

In this scenario, the injection of pure CO_2 at a lower temperature into a vertical wellbore containing pure CO_2 is simulated. The information of the simulation case is given in Table 1, and the final pressure and temperature profiles obtained from DARTS-well are compared with those from OLGA, as shown in Figure 2.

Table 1—Information of the non-isothermal single-phase (gas) single-component (CO_2) fluid flow in a vertical wellbore.

Wellbore Geometry	**Inclination angle: 0 (Vertical wellbore)** **Total length: 1 km (20 segments, each segment 50 meters)** **Diameter: 0.1 m** **Wall absolute roughness: 2.5 × 10^{-5} m**
Fluid Properties	Injected fluid composition: Pure CO_2 Wellbore initial fluid composition: Pure CO_2 Density: Peng-Robinson EoS Enthalpy: Peng-Robinson EoS Viscosity: Fenghour et al. (1998)
Initial Conditions	Wellhead pressure: 5 bar Wellhead temperature: 25° C Geothermal gradient: 25°C/km Fluid at rest (i.e., v_{fluid} = 0m/s)
Boundary Conditions	**At wellhead:** Injection rate: 2 kg/s Injection temperature: 20° C (constant) Injected fluid composition: Given in Fluid Properties **At bottom-hole (perforation):** Reservoir permeability: 115 mD Perforation hole diameter: 2 cm Reservoir pressure: Equal to the initial pressure of the lowermost segment Reservoir thickness: Equal to the length of the lowermost segment Skin factor: 0
Simulation Schedule	Duration: 10 minutes

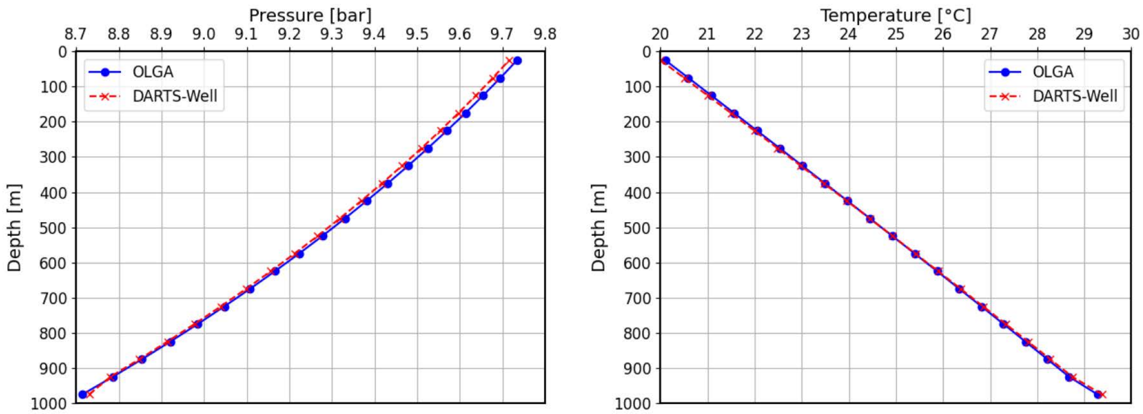

(a) Pressure profiles. (b) Temperature profiles.

Figure 2—Comparison of pressure and temperature profiles of DARTS-well with OLGA for the non-isothermal singlephase single-component model.

Isothermal two-phase (gas and liquid) two-component (CO_2 and H_2O) fluid flow in a vertical wellbore

In this scenario, the injection of impure gaseous CO_2 into a vertical wellbore containing a column of water is simulated. The information of the simulation case is given in Table 2. The final pressure and liquid hold-up profiles obtained from DARTS-well are compared with those from OLGA, as shown in Figure 3. The difference in segment liquid hold-ups observed in Subfigure 3-b arises from the distinct mathematical formulations for two-phase fluid flow employed by DARTS-well (DFM model) and OLGA (MFM model).

Table 2—Information of the isothermal two-phase (gas and liquid) two-component (CO_2 and H_2O) fluid flow in a vertical wellbore.

Wellbore Geometry	**Inclination angle: 0 (Vertical wellbore)** **Total length: 1 km (20 segments, each segment 50 meters)** **Diameter: 0.1 m** **Wall absolute roughness: 2.5×10^{-5} m**
Fluid Properties	Injected fluid composition: Impure CO_2 (99% CO_2, 1% H_2O) Wellbore initial fluid composition: Water CO_2-rich phase density: Peng-Robinson EoS Aqueous phase density: Garcia (2001) CO_2-rich phase viscosity: Fenghour et al. (1998) Aqueous phase viscosity: Islam and Carlson (2012) Relative permeability: Brooks and Corey model ($n_{gas} = 2$ and $n_{liquid} = 2$) Gas-liquid IFT: Macleod-Sugden surface tension model
Initial Conditions	Wellhead pressure: 5 bar System temperature: 25°C (constant) Wellbore initial fluid composition: Given in Fluid Properties Fluid at rest (i.e., $v_{fluid} = 0$m/s)
Boundary Conditions	**At wellhead:** Injection rate: 2 kg/s Injection temperature: System temperature Injected fluid composition: Given in Fluid Properties **At bottom-hole (perforation):** Reservoir permeability: 200 mD Perforation hole diameter: 2 cm Reservoir pressure: Equal to the initial pressure of the lowermost segment Reservoir thickness: Equal to the length of the lowermost segment Skin factor: 0
Simulation Schedule	Duration: 100 seconds

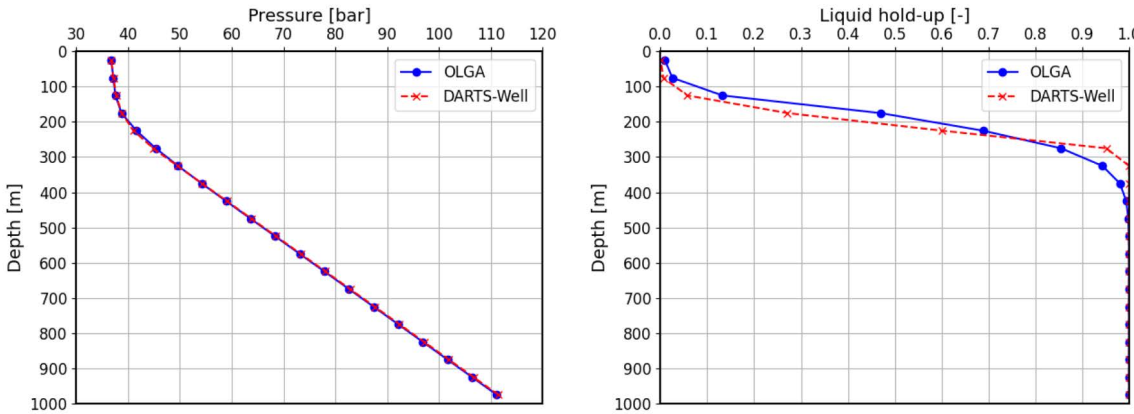

(a) Pressure profiles. (b) Liquid hold-up profiles.

Figure 3—Comparison of pressure and liquid hold-up profiles of DARTS-well with OLGA for the isothermal two-phase two-component fluid flow in a vertical wellbore.

Isothermal two-phase (gas and liquid) two-component (CO_2 and H_2O) fluid flow in an inclined wellbore

This scenario is the same as the previous one, except that the wellbore is inclined at 45 degrees. The total length of the wellbore is still 1 km, which means that in this case, the true vertical depth of the wellbore is 1000 × cos 45° (≈ 707.1 m). The final pressure and liquid hold-up profiles obtained from DARTS-well are compared

with those from OLGA, as shown in Figure 4. Note that the vertical axis in Figure 4 is a measured depth. As in the case of Subfigure 3-b, the difference in liquid hold-ups in Subfigure 4-b is also caused by the difference in mathematical formulations employed.

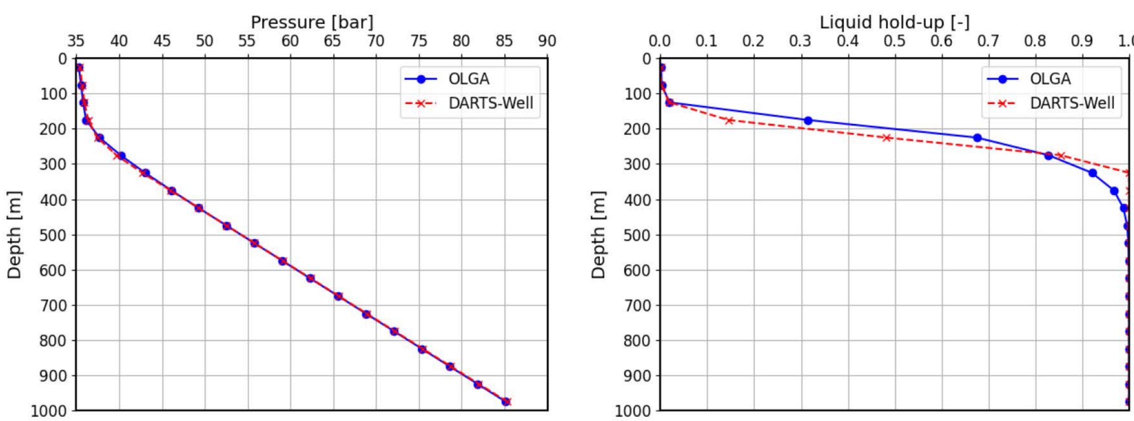

(a) Pressure profiles. (b) Liquid hold-up profiles.

Figure 4—Comparison of pressure and liquid hold-up profiles of DARTS-well with OLGA for the isothermal two-phase two-component fluid flow in an inclined wellbore.

Coupled wellbore-reservoir study

In this section, the developed coupled wellbore-reservoir model is used to simulate the injection of pure dry CO_2 into a depleted reservoir containing methane and connate water. This test case is inspired by the PORTHOS project, which involves CO_2 injection into an offshore depleted hydrocarbon field in the North Sea near the Netherlands (https://www.porthosco2.nl/en/). The wellbore and reservoir properties used in the simulation are listed in Table 3.

Table 3—Information of the injection of CO2 into a depleted hydrocarbon reservoir via a multi-segmented wellbore.

Wellbore Geometry	**Inclination angle: 0 (Vertical wellbore)** **Total length: 3 km (60 segments, each segment 50 meters)** **Diameter: 0.1 m** **Wall absolute roughness: 2.5×10^{-5} m**
Reservoir Geometry	Grid type: A cylindrical grid Thickness: 250 meters (5 cells, each cell 50 meters) Radius: 1000 meters Reservoir top depth: 2850 meters
Reservoir Rock Properties	Porosity: 0.2 Horizontal and vertical permeability: 20 and 2 mD, respectively Rock compressibility: 0 bar^{-1}
Fluid Properties	Flash calculations: To calculate phase compositions and saturations, a two-phase flash which is based on a combination of the Peng-Robinson cubic equation of state (PR-EOS) for the hydrocarbon/CO_2-rich phase and an activity model for the aqueous phase is used, which is available in DARTS-flash (Wapperom and Voskov, 2024). Reservoir initial fluid composition: 25% connate water saturation and 75% CH4 Wellbore initial fluid composition: Pure CH4 Injected fluid composition: Pure CO_2 Density of CO_2/CH_4-rich phase: Peng-Robinson EoS Aqueous phase density: Garcia (2001) Viscosity of CO_2/CH_4-rich phase: Fenghour et al. (1998) Viscosity of aqueous phase: Islam and Carlson (2012) Relative permeability: Brooks and Corey model ($n_{gas} = 4$ and $n_{water} = 1.5$) Gas-liquid IFT: Macleod-Sugden surface tension model
Initial Conditions	Wellhead pressure: 20 bar Reservoir pressure: Equal to the initial pressure of the lowermost segment which is 24.2 bar System temperature: 35°C (constant) Reservoir and wellbore initial fluid composition: Given in Fluid Properties Fluid at rest (i.e., $\upsilon_{fluid} = 0$m/s)
Boundary Conditions	**At wellhead:** Injection rate: 30 kg/s Injection temperature: System temperature Injected fluid composition: Given in Fluid Properties **At reservoir boundaries:** No flow at uppermost and lowermost boundaries, and constant pressure at radial boundaries using infinitely large grid cells.
Simulation Schedule	Duration: 1 year

The profiles of pressure and overall mole fraction of CH_4 along the wellbore are plotted over time in Figure 6, and the reservoir fluid properties distribution after 1 year of injection are shown in Figure 5. As shown in Figure 6-b, as the injection commences, the injected CO_2 pushes the methane present in the wellbore into the reservoir. This increases CH_4 concentration in the reservoir, which can hardly be observed after 1 year of injection in Figure 5 due to the small volume of CH_4 initially in the wellbore. The CH_4 concentration increase is more pronounced at the beginning of injection between the intact reservoir and the front of the injected CO_2.

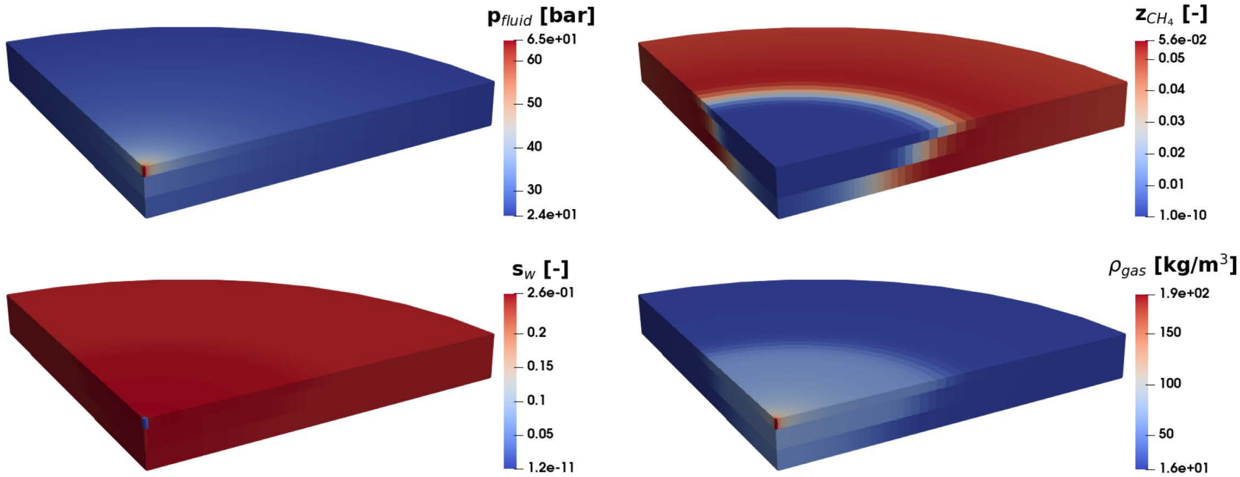

Figure 5—Reservoir fluid properties, including p_{fluid} (fluid pressure), z_{CH_4} (overall mole fraction of CH_4), s_w (saturation of the aqueous phase), and ρ_{gas} (density of the CO_2/CH_4-rich phase) after 1 year of CO_2 injection. The cylindrical reservoir is visualized by clipping it to one-quarter of its horizontal extent and half of its vertical extent to enhance the clarity of the results.

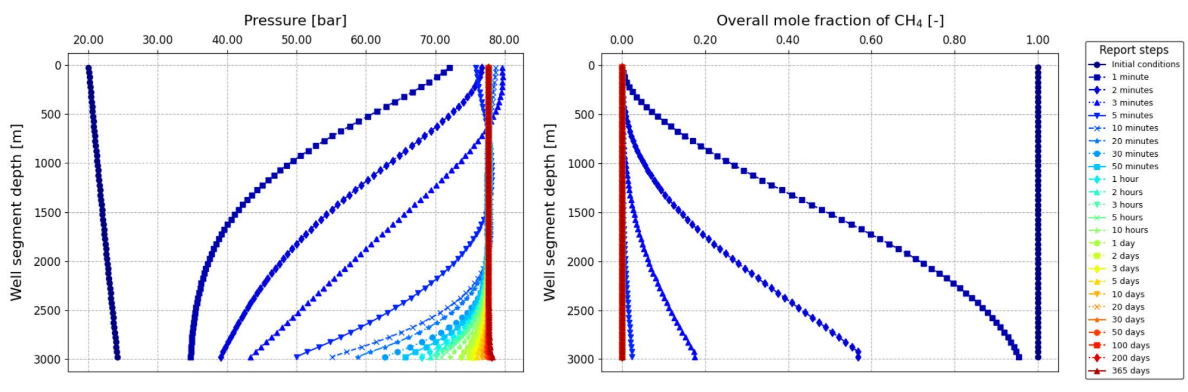

(a) Pressure profiles. (b) CH_4 overall mole fraction profiles.

Figure 6—Profiles of pressure and CH_4 overall mole fraction along the wellbore over time.

As shown in Figure 6-a, as injection starts, pressure does not build up instantly in the wellbore which is because of the fluid (methane) compressibility. This effect is even more outstanding in the reservoir due to the large pore volume available in the depleted reservoir. After a sufficiently long period of injection, as the reservoir pressure increases, the bottom-hole pressure will be affected, but this is not observed during the injection period in the first year.

By examining the evolution of water saturation (s_w), it can be inferred that after one year of injection, as shown in Figure 5, water vaporization is observed in the reservoir grid cells near the wellbore, resulting in the complete depletion of water in reservoir cells near the perforation (dry-out region), but the evaporation front is significantly farther behind the injected CO_2 front. The evolution of the density of the CO_2/CH_4-rich phase (ρ_{gas}) shows that the phase density increases over time because of two reasons. First, CH_4 initially in-place has a low density compared to the injected CO_2. Therefore, as the CO_2 displaces CH_4 in the reservoir, the density increases. Second, pressure build-up in the reservoir also increases the phase density, particularly for CO_2 because of having conditions near its liquid state.

Regarding computational performance, ramp-up time step sizes are used at the beginning with a maximum time step size of 100 minutes. During the initial two days of injection, the computational effort is higher because the solver requires two or more Newton-Raphson iterations per time step to achieve convergence and sometimes requires time step cuts due to significant pressure changes in the wellbore and near-wellbore region. Beyond this period, as pressure stabilizes, only a single iteration per time step is sufficient for convergence.

Conclusions

This study presents the development and validation of DARTS-well, a coupled wellbore-reservoir model tailored for subsurface CO_2 sequestration applications. The model addresses the limitations of traditional reservoir simulators by incorporating a multi-segment multiphase wellbore simulation using the Drift-Flux Model (DFM) and full thermodynamic model. The integration with the Delft Advanced Research Terra Simulator (DARTS) through Operator-Based Linearization (OBL) ensures computational efficiency and robust handling of complex

physics in CCS operations. Validation against the commercial simulator OLGA demonstrates the model's accuracy for various CO_2 injection scenarios, including single-phase and two-phase flows in vertical and inclined wellbores. Results from the realistic coupled wellbore-reservoir model highlight the formulation capability to capture critical wellbore-reservoir interactions, particularly interplay between different thermodynamic properties, offering a step toward improved modeling of CO_2 injection processes. The work provides a useful tool for further studies aimed at better understanding and managing CO_2 sequestration operations in subsurface reservoirs.

Acknowledgements

We want to acknowledge the financial support of the ASSET program by Shell Global Solutions International. We thank the DARTS research group for valuable discussions for implementation of the code. We also thank Curtis Oldenburg for his assistance in clarifying several concepts of the DFM model.

References

Abdelaal, M. and Zeidouni, M. (2023). Coupled wellbore-reservoir modelling to evaluate CO2 injection rate distribution over thick multilayer storage zones. *International Journal of Greenhouse Gas Control*, **129**:103–987.

Ahusborde, E., Amaziane, B., de Hoop, S., El Ossmani, M., Flauraud, E., Hamon, F. P., Kern, M., Socie, A., Su, D., Mayer, K., Toth, M., and Voskov, D. (2024). A benchmark study on reactive two-phase flow in porous media: Part ii - results and discussion. *Computational Geosciences*, **28**(3):395–412.

Cai, Y., Yang, D., Feng, G., and Lei, H. (2024). Transient H2O-CO2 wellbore leakage under evolving recharge conditions considering CO2 phase change. *Journal of Cleaner Production*, **450**:141–942.

Castaneda, J. R., Kahrobaei, S., Aghajanloo, M., Voskov, D., and Farajzadeh, R. (2025). Numerical and experimental investigation of impact of CO2 hydrates on rock permeability. *Fuel*, **381**:133–708.

Ertekin, T., Abou-Kassem, J. H., and King, G. R. (2001). Basic applied reservoir simulation. (No Title).

Feng, G., Xu, T., Tian, H., Lu, M., Connell, L. D., Lei, H., and Shi, Y. (2017). Three-phase non-isothermal flow behavior of CO2-brine leakage from wellbores. *International Journal of Greenhouse Gas Control*, **64**:183–193.

Fenghour, A., Wakeham, W. A., and Vesovic, V. (1998). The viscosity of carbon dioxide. *Journal of physical and chemical reference data*, **27**(1):31–44.

Garcia, J. E. (2001). Density of aqueous solutions of CO2.

Goda, H., Hibiki, T., Kim, S., Ishii, M., and Uhle, J. (2003). Drift-flux model for downward two-phase flow. *International journal of heat and mass transfer*, **46**(25):4835–4844.

Hammer, M., Deng, H., Liu, L., Langsholt, M., and Munkejord, S. T. (2021). Upward and downward two-phase flow of CO2 in a pipe: Comparison between experimental data and model predictions. *International Journal of Multiphase Flow*, **138**:103–590.

Hu, L., Pan, L., and Zhang, K. (2012). Modeling brine leakage to shallow aquifer through an open wellbore using t2well/eco2n. *International Journal of Greenhouse Gas Control*, **9**:393–401.

Indina, V., Fernandes, B., Delshad, M., Farajzadeh, R., and Sepehrnoori, K. (2024). On the significance of hydrate formation/dissociation during CO2 injection in depleted gas reservoirs. In SPE EOR Conference at Oil and Gas West Asia, page D021S013R001. SPE.

Islam, A. W. and Carlson, E. S. (2012). Viscosity models and effects of dissolved CO2. *Energy & fuels*, **26**(8):5330–5336.

Khait, M. and Voskov, D. V. (2017). Operator-based linearization for general purpose reservoir simulation. *Journal of Petroleum Science and Engineering*, **157**:990–998.

Livescu, S., Durlofsky, L., Aziz, K., and Ginestra, J. (2010). A fully-coupled thermal multiphase wellbore flow model for use in reservoirsimulation. *Journalof Petroleum Science and Engineering*, **71**(3-4):138–146.

Moridis, G. J., Reagan, M. T., and Liu, Y. (2022). Numerical simulations in support of a long-term test of gas production from hydrate accumulations on the alaska north slope: Reservoir response to interruptions of production (shut-ins). *Energy andFuels*, **36**(7):3496–3525.

Oldenburg, C. M. and Pan, L. (2020). Major CO2 blowouts from offshore wells are strongly attenuated in water deeper than 50 m. *Greenhouse Gases: Science and Technology*, **10**(1):15–31.

Pan, L. (2011). T2well/eco2n version 1.0: multiphase and non-isothermal model for coupled wellbore-reservoir flow of carbon dioxide and variable salinity water.

Pan, L. and Oldenburg, C. (2020). Mechanistic modeling of CO2 well leakage in a generic abandoned well through a bridge plug cement-casing gap. *International Journal of Greenhouse Gas Control*, **97**:103025.

Pan, L. and Oldenburg, C. M. (2014). T2well—an integrated wellbore-reservoir simulator. *Computers & Geosciences*, **65**:46–55.

Pan, L., Oldenburg, C. M., Pruess, K., and Wu, Y.-S. (2011a). Transient CO2 leakage and injection in wellbore-reservoir systems for geologic carbon sequestration. *Greenhouse Gases: Science and Technology*, **1**(4):335–350.

Pan, L., Webb, S. W., and Oldenburg, C. M. (2011b). Analytical solution for two-phase flow in a wellbore using the drift-flux model. *Advances in Water Resources*, **34**(12):1656–1665.

Pour, K. M., Voskov, D., and Bruhn, D. (2023). Coupled modeling of well and reservoir for geo-energy applications. *Geoenergy Science and Engineering*, 227.

Rasmusson, K., Tsang, C.-F., Tsang, Y., Rasmusson, M., Pan, L., Fagerlund, F., Bensabat, J., and Niemi, A. (2015). Distribution of injected CO2 in a stratified saline reservoir accounting for coupled wellbore-reservoir flow. *Greenhouse Gases: Science and Technology*, **5**(4):419–436.

Shi, H., Holmes, J. A., Durlofsky, L. J., Aziz, K., Diaz, L., Alkaya, B., and Oddie, G. (2005). Drift-flux modeling of two-phase flow in wellbores. *Spe Journal*, **10**(01):24–33.

Spesivtsev, P., Sinkov, K., and Osiptsov, A. (2013). Comparison of drift-flux and multi-fluid approaches to modeling of multiphase flow in oil and gas wells. *WIT Transactions on Engineering Sciences*, **79**:89–99.

Tonkin, R., O'Sullivan, J., Gravatt, M., and O'Sullivan, M. (2023). A transient geothermal wellbore simulator. *Geothermics*, **110**:102–653.

Van Nimwegen, A., Peters, E., Gargar, N. K., and Hurter, S. (2023). Cold CO2 injection in depleted gas fields: Coupling of wellbore and reservoir. In The Fourth EAGE Global Energy Transition Conference and Exhibition, volume **2023**, pages 1–5. European Association of Geoscientists & Engineers.

Voskov, D. V. (2017). Operator-based linearization approach for modeling of multiphase multi-component flow in porous media. *Journal of Computational Physics*, **337**:275–288.

Wang, Y., Voskov, D., Khait, M., and Bruhn, D. (2020). An efficient numerical simulator for geothermal simulation: A benchmark study. *Applied Energy*, 264.

Wapperom, M., Tian, X., Novikov, A., and Voskov, D. (2024). FluidFlower Benchmark: Lessons Learned from the Perspective of Subsurface Simulation. *Transport in Porous Media*, **151**(5):1033–1052.

Wapperom, M. and Voskov, D. (2024). Darts-flash: an open-source thermodynamic modelling software for experimental and numerical study of subsurface energy transition applications. In Fifth EAGE Global Energy Transition Conference & Exhibition (GET 2024), volume **2024**, pages 1–5. European Association of Geoscientists & Engineers.

Zamani, N., Oldenburg, C. M., Solbakken, J., Aarra, M. G., Kowollik, P., Alkan, H., Amro, M. M., Nassan, T. H., Estrada, J. K., and Burachok, O. (2024). CO2 flow modeling in a coupled wellbore and aquifer system: Details of pressure, temperature, and dry-out. *International Journal of Greenhouse Gas Control*, **132**:104067.